Thermochimica Acta, 157 (1990) 347–355
Elsevier Science Publishers B.V., Amsterdam – Printed in The Netherlands

THE HIGH TEMPERATURE OXIDATION OF FeV_2O_4

P.P. STANDER

Council for Mineral Technology (MINTEK); Private Bag X3015,
Randburg 2125 (Republic of South Africa)

C.P.J. VAN VUUREN *

Department of Chemistry, University of Pretoria, Pretoria 0002 (Republic of South Africa)

(Received 12 June 1989)

ABSTRACT

The high temperature oxidation of FeV_2O_4 was investigated by means of thermoanalytical techniques and X-ray powder diffraction. FeV_2O_4 is oxidized to $FeVO_4$ and V_2O_5 through intermediates such as R_2O_3 (a solid solution of α-Fe_2O_3 and V_2O_3), VO_2, V_6O_{13} and FeV_2O_6. Depending on the heating rate, self-heating due to exothermic processes inhibits oxidation by the formation of a V_2O_5 crust.

INTRODUCTION

Vanadium is present in titaniferous magnetite ore as V^{3+} in a spinel mineral coulsonite, i.e. FeV_2O_4, which is formed by replacement of Fe^{3+} in magnetite by V^{3+} [1].

A well known roast–leach process is employed in the production of V_2O_5 and NH_4VO_3 from titaniferous magnetite ore. According to Gabra et al. [2] this process involves the following basic chemistry in the presence of Na_2CO_3:

(1) oxidation of the ore: $V^{3+}, Cr^{3+}, Fe^{2+} \rightarrow V^{5+}, Cr^{6+}, Fe^{3+}$;

(2) $M_xO_y + zNa_2CO_3 \rightarrow zNa_2O \cdot M_xO_y + zCO_2$.

Because of the basicity of Na_2CO_3 and the fact that V_2O_5 is the most acidic oxide in the ore, sodium vanadates should preferably be formed on the basis of the Lux–Flood acid–base theory. These vanadates are water soluble and can be leached from the ore. In practice, however, sodium chromates, aluminates and silicates also form, and are extracted during the leaching process together with the sodium vanadates.

---

* Correspondence should be addressed to this author at P.O. Box 904399, Faerie Glen 0043, Pretoria, Republic of South Africa.

0040-6031/90/$03.50

The minimization of Al, Si and Cr extraction by controlling parameters such as roasting temperature, roasting time, sodium salt concentration, etc., is a well developed art rather than a science. Optimum roasting conditions are not founded on a thorough understanding of the fundamental chemistry involved in the reaction of FeV_2O_4 with the sodium salt, as well as the reaction of the other oxides with the sodium salt used. In view of this, a fundamental study of the oxidation of FeV_2O_4 in mixtures of Na_2CO_3 and Na_2SO_4 (the basic salts most commonly used) was conducted.

As a starting point, the high temperature oxidation of FeV_2O_4 was investigated. From a mechanistic point of view, it is important to know which oxidation products are formed and at which temperature such products would be present in the FeV_2O_4–Na_2CO_3 and FeV_2O_4–Na_2SO_4 systems. The present paper deals with this subject.

Ryzhov et al. [3] studied the oxidation of FeV_2O_4 at high temperatures and proposed the following mechanism of oxidation

$$\begin{aligned} &FeV_2O_4 \rightarrow FeV_2O_4 + R_2O_3 \rightarrow FeV_2O_4 + R_2O_3 + FeVO_4 \\ &\qquad \rightarrow FeVO_4 + V_2O_5 + R_2O_3 \end{aligned}$$

The existence of R_2O_3 (a solid solution of α-Fe_2O_3 and V_2O_3) implies an incomplete oxidation of the spinel. Vatolin et al. [4] investigated the mechanism of oxidation of FeV_2O_4 and proposed the following mechanism of oxidation

$$\begin{aligned} &FeV_2O \rightarrow R_2O_3(1) + R_2O_3(2) + FeVO_4 \rightarrow R_2O_3(3) + FeVO_4 + V_2O_5 \\ &\qquad \rightarrow Fe_2O_3 + V_2O_5 \end{aligned}$$

(1), (2) and (3) indicate variable composition phases.

Burdese [5] constructed a ternary phase diagram for the system FeO–VO–O_2 at 600 °C. According to this phase diagram, the oxidation of FeV_2O_4 would proceed as follows

$$\begin{aligned} &FeV_2O_4 \rightarrow Fe_3O_4 + Fe_2O_3 + V_2O_3 \rightarrow V_2O_3 + Fe_2O_3 \\ &\qquad \rightarrow VO_2 + V_2O_3 + Fe_2O_3 \rightarrow VO_2 + Fe_2O_3 \rightarrow V_6O_{13} + Fe_2O_3 \\ &\qquad \rightarrow FeV_2O_6 + V_6O_{13} + FeVO_4 \rightarrow V_2O_5 + FeVO_4 \end{aligned}$$

There are distinct differences in the mechanisms proposed by these workers. In addition to the fact that the mechanism of oxidation is not clear, no DTA, DSC or dynamic TG information is available for the high temperature oxidation of FeV_2O_4.

EXPERIMENTAL

Sample preparation

The method of Rogers et al. [6] was used to prepare FeV_2O_4. This method consists of the following steps: (i) a 2 : 1 stoichiometric mixture of V_2O_3 and

Fe_2O_3 is ground to form a homogeneous mixture. However, in this study, the two oxides were stirred in petroleum ether for ≈ 18 h; (ii) the mixture is heated in a resistively heated tube furnace at 1100 °C under a 4.5 : 1 $CO-CO_2$ dynamic atmosphere. This temperature, as well as the atmospheric conditions, is maintained for 24 h; (iii) the FeV_2O_4 is cooled to ambient temperatures in the $CO-CO_2$ atmosphere and is subsequently checked for unreacted Fe_2O_3 and V_2O_3 by X-ray powder diffraction (XRPD) (iv) steps (ii) and (iii) are repeated until no starting materials are detected. The total reaction time needed was found to be 48 h (stirred mixture) or 72 h (ground mixture).

The FeV_2O_4 prepared was characterized by means of Mössbauer spectroscopy and XRPD. The XRPD pattern obtained corresponds with that of Gupta and Mathur [7]. A cubic unit cell constant of 8.454 Å was obtained for this spinel, comparing well with values of 8.45–8.46 Å reported by most other workers. The room temperature Mössbauer spectrum obtained consists of a singlet ($\delta = 0.87$ mm s^{-1}) and a doublet ($\delta = 0.26$ mm s^{-1}) which are both assignable to Fe^{2+} in T_d co-ordination according to Riedel and Anik [8]. No significant traces of Fe^{3+} could be detected by the Mössbauer study.

Thermal analysis

TG experiments were carried out on a DuPont 990 thermal analyser with a 951 TG analyser unit. In all isothermal runs, the sample was inserted into the TG furnace only after the furnace had reached the predetermined isothermal temperature. All DSC runs in this study were recorded on a Perkin–Elmer DTA 1700 operated in the DSC mode; Pt sample and reference cups were used. All thermal analysis runs were recorded in a dynamic atmosphere of pure O_2, with a flow rate of ≈ 50 ml min^{-1}.

X-ray powder diffraction analysis

All XRPD patterns were recorded on a Seifert MZ-IV instrument using Cu $K\alpha$ radiation.

RESULTS AND DISCUSSION

Isothermal studies

Temperature range 360–380 °C

In this temperature range, very slow oxidation, starting at a maximum rate, was observed (Fig. 1a, curves 1 and 2). XRPD patterns obtained after 20 h of oxidation at this temperature revealed the presence of α-Fe_2O_3 and

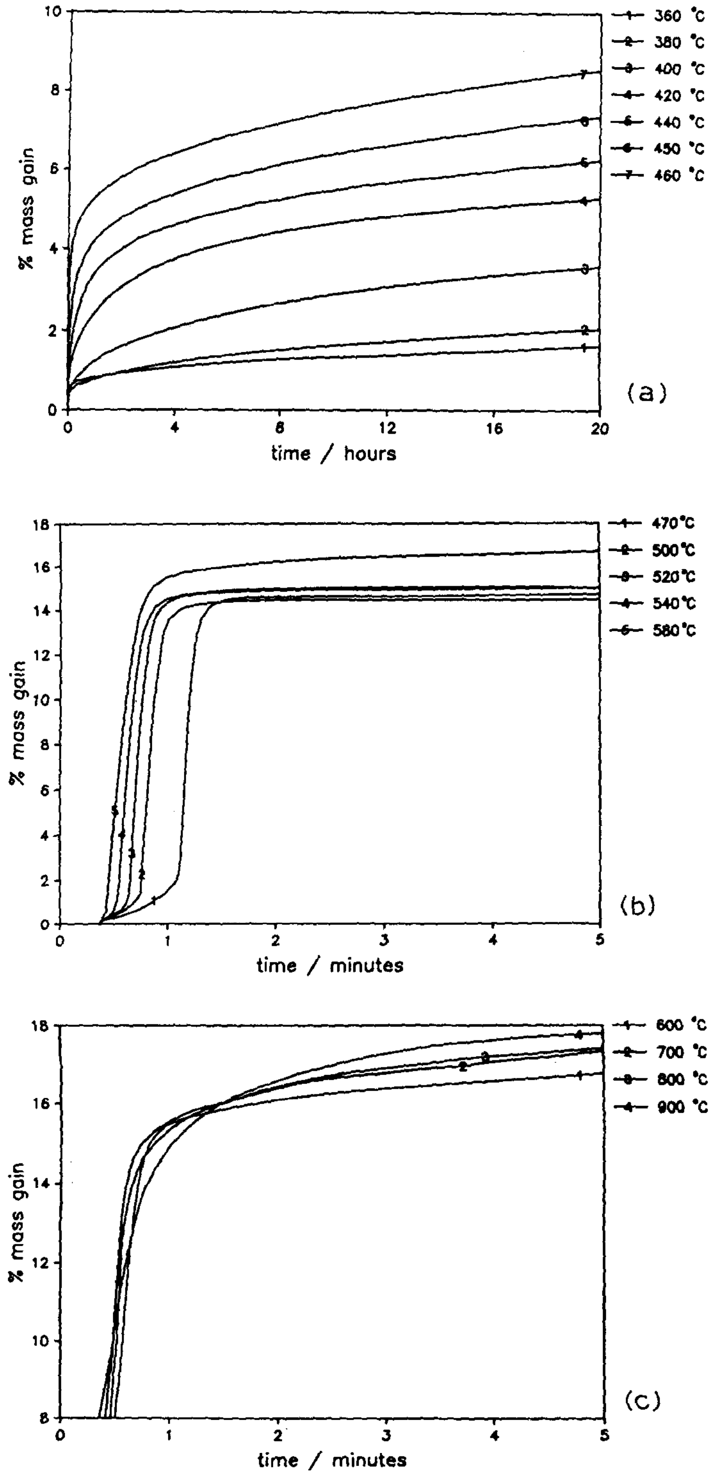

Fig. 1. Isothermal TG curves for the oxidation of FeV_2O_4 in O_2 in the temperature range 360–900 ° C.

V_2O_3 and high concentrations of FeV_2O_4. No V_2O_5 or any other vanadium oxide could be detected.

According to the study of Baiker et al. [9], and the results of this study, on the oxidation of V_2O_3 powder, V_2O_3 is oxidized to V_2O_5 in the temperature range ≈100–370 °C. The fact that V_2O_3 XRPD lines are observed at temperatures as high as 380 °C suggests the formation of some type of solid solution of V_2O_3 and α-Fe_2O_3. Amirova et al. [10] prepared such solid solutions, i.e. $Fe_{2(1-x)}V_{2x}O_3$ with $x \in [0, 1]$, and found that these solid solutions are of a single phase with rhombohedral structure. The formation of such a solid solution with $x = 2/3$ could be realized by the following solid state reaction

$$\tfrac{2}{3}FeV_2O_4 + \tfrac{1}{6}O_2 \rightarrow Fe_{0.67}V_{1.33}O_3 \qquad (1)$$

Ryzhov et al. [3] and Vatolin et al. [4] also described the formation of an R_2O_3 ($R = Fe$, V) solid solution as the initial step in the oxidation of FeV_2O_4.

Temperature range 400–460 °C

In this temperature range, very slow oxidation of FeV_2O_4 prevails (Fig. 1a, curves 3 to 7). XRPD revealed the presence of R_2O_3 ($R = Fe$, V), VO_2 and V_2O_5 and high concentrations of FeV_2O_4. The formation of VO_2 and V_2O_5 from the oxidation of the solid solution can be presented by the following solid state reactions

$$Fe_{2(1-x)}V_{2x}O_3 + \frac{(x+3)}{2}O_2 \rightarrow 2xVO_2 + (1-x)Fe_2O_3 \qquad (2)$$

$$2VO_2 + \tfrac{1}{2}O_2 \rightarrow V_2O_5 \qquad (3)$$

The low rate of oxidation as observed from Fig. 1, curves 3 to 7 is therefore a result of the incomplete conversion of FeV_2O_4 to the R_2O_3 solid solution. The total reaction, although incomplete conversion of FeV_2O_4 takes place, can therefore be represented as

$$FeV_2O_4 + \tfrac{5}{4}O_2 \rightarrow V_2O_5 + \tfrac{1}{2}Fe_2O_3 \qquad (4)$$

The fact that V_2O_5 is the first pentavalent vanadium oxide observed in the oxidation of FeV_2O_4, and not $FeVO_4$ (iron orthovanadate), is contradictory with the mechanisms proposed by Ryzhov et al. [3] and Vatolin et al. [4], who found $FeVO_4$ formed before V_2O_5. The formation of VO_2 was not observed by Ryzhov et al. [3] and Vatolin et al. [4], but it is predicted by the FeO–VO–O phase diagram of Burdese [11] and by studies on the mechanism of oxidation of V_2O_3 [9,12].

Temperature range 470–580 °C

In strong contrast to the very slow rates of oxidation at $T < 460$ °C, extremely fast oxidation of FeV_2O_4, leading to a 14.48–14.88% mass gain, was observed in this temperature range. This implies 81–83% oxidation of the spinel. Representative TG curves are shown in Fig. 1b.

XRPD analysis verified the formation of FeV_2O_6, V_6O_{13}, V_2O_5, $FeVO_4$ and the R_2O_3 solid solution. It is anticipated, however, that the V_2O_3 content of the solid solution will be very low. It is important to note that the reaction is completed within 5 min.

The fact that incomplete oxidation of FeV_2O_4 takes place can be explained by the fact that the exothermic processes cause severe self-heating, which causes the V_2O_5 formed to be heated to above its melting point at 670 °C. The molten V_2O_5 solidifies as the reaction slows down. This causes a V_2O_5 crust to form, which reduces the O_2 availability for further oxidation.

FeV_2O_6 is probably formed from the direct oxidation of FeV_2O_4

$$FeV_2O_4 + O_2 \rightarrow FeV_2O_6 \qquad (5)$$

The formation of V_6O_{13}, $FeVO_4$, V_2O_5 and α-Fe_2O_3 from redox reactions or decomposition reactions of FeV_2O_6 could be realized by several solid state reactions

$$FeV_2O_6 + \tfrac{1}{12}O_2 \rightarrow \tfrac{1}{6}V_6O_{13} + FeVO_4 \qquad (6)$$

$$FeV_2O_6 + (\tfrac{1}{4} - x)O_2 \rightarrow xV_6O_{13} + FeVO_4 + (\tfrac{1}{2} - x)V_2O_5 \quad (0 \leqslant x \leqslant \tfrac{1}{4}) \qquad (7)$$

$$FeV_2O_6 + \tfrac{1}{4}V_6O_{13} + \tfrac{1}{2}Fe_2O_3 + \tfrac{1}{4}V_2O_5 \qquad (8)$$

$FeVO_4$, V_6O_{13} and V_2O_5 could also be formed via the following solid state reactions

$$\tfrac{1}{2}Fe_2O_3 + \tfrac{1}{2}V_2O_5 + FeVO_4 \qquad (9)$$

$$3V_2O_3 + 2O_2 \rightarrow V_6O_{13} \qquad (10)$$

$$\tfrac{1}{3}V_6O_{13} + \tfrac{1}{3}O_2 \rightarrow V_2O_5 \qquad (11)$$

Temperature range 600–900 °C

In this temperature range, complete oxidation of FeV_2O_4 was observed (Fig. 1c). The experimentally observed mass gain of 17.95 ± 0.05% is in good agreement with the theoretical mass gain of 18.04%.

Ryzhov et al. [3] did not observe complete oxidation of FeV_2O_4, even at elevated temperatures. They ascribed this to the stability of R_2O_3 at these high temperatures. The maximum degree of oxidation observed by these workers was 70%. In contrast with this, it was observed that at 900 °C, FeV_2O_4 is completely oxidized within 10 min. Vatolin et al. [4] also observed complete oxidation of FeV_2O_4.

In this study, the final product of oxidation was found to be a 2 : 1 molar mixture of $FeVO_4$ and V_2O_5, which is in agreement with the phase diagram of Burdese [11], but contradictory to the findings of Ryzhov et al. [3] and Vatolin et al. [4].

The total oxidation reaction is therefore

$$FeV_2O_4 + \tfrac{5}{4}O_2 \rightarrow FeVO_4 + \tfrac{1}{2}V_2O_5 \qquad (12)$$

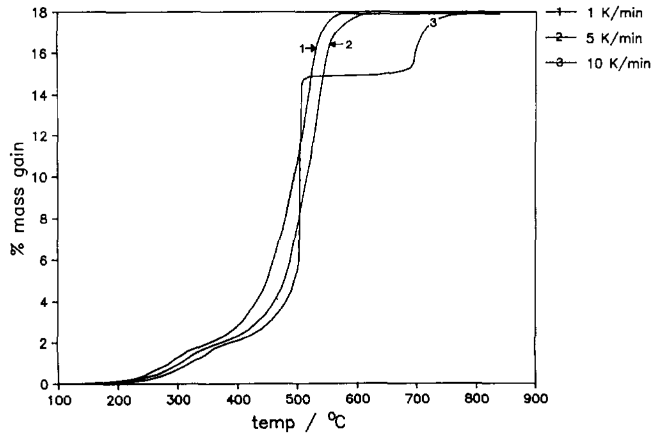

Fig. 2. Dynamic TG curves for the oxidation of FeV_2O_4 in O_2 at heating rates of 1, 5 and 10 K min^{-1}.

Dynamic studies

From the TG curves (Fig. 2) for the oxidation of FeV_2O_4 in pure O_2, it is clear that the shape of the TG curve is influenced to a large extent by the heating rate to which FeV_2O_4 is subjected.

At heating rates $\geqslant 10\,^{\circ}C\ min^{-1}$, a plateau appears at 14.48–14.88% mass gain. The very steep mass gain at $T \approx 520\,^{\circ}C$ in curve 3 of Fig. 2 is caused by self-heating. Further oxidation from $\approx 670\,^{\circ}C$ as the V_2O_5 crust melts is further support for the fact that resistance to complete oxidation in the 500–670 °C temperature range is a purely physical restriction brought about by a V_2O_5 crust, as discussed earlier. This is in agreement with the fact that oxidation is complete at much lower temperatures at low heating rates (curves 1 and 2), where sample self-heating is not significant. The plateau at 500–670 °C (curve 3) therefore supports the observations made under isothermal conditions.

Stopping dynamic runs at different stages of oxidation at various heating rates, and running XRPD patterns, showed the following. At 2.00% mass gain, FeV_2O_4 and R_2O_3 (R = Fe, V) are the only substances present, while at $\approx 14.5\%$ mass gain (curve 3) FeV_2O_6, $FeVO_4$, VO_2, V_6O_{13} and R_2O_3 are present. At both low and high heating rates, the final products of oxidation are $FeVO_4$ and V_2O_5.

DSC and DTA

The various DSC peaks in Fig. 3 are assigned as follows: (1) formation of the R_2O_3 (R = Fe, V) solid solution; (2) oxidation of the solid solution and oxidation of the remaining spinel. (The end of these exothermic process corresponds with a 14.44–14.88% mass gain); (3) melting of V_2O_5; (4) exothermic oxidation of the incompletely oxidized oxides such as V_6O_{13} and

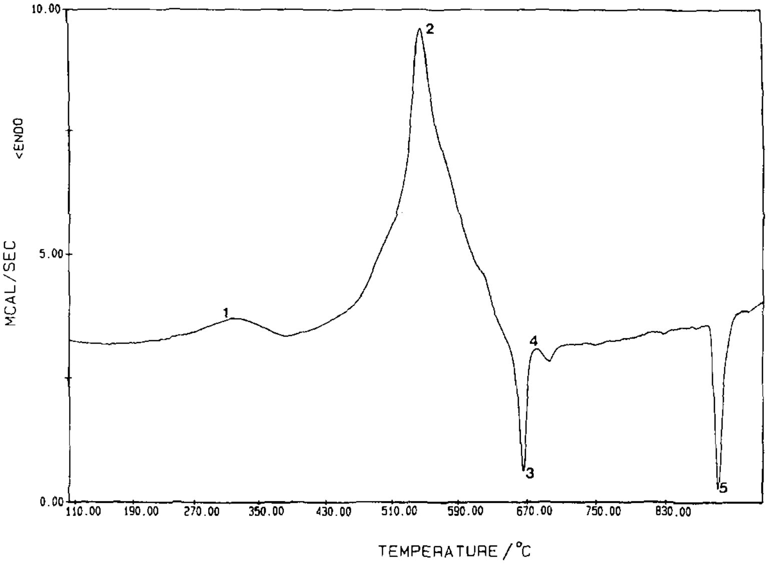

Fig. 3. DSC curve for the oxidation of FeV_2O_4 in O_2 at a heating rate of 10 K min^{-1}.

FeV_2O_6. (Note that this exothermic process overlaps with the melting of V_2O_5, which goes through a minimum at ≈ 674 °C); (5) melting of $FeVO_4$ at 875 °C (onset) and 890 °C (peak minimum).

From the fact that 1 mol of $FeVO_4$ is formed per mol of FeV_2O_4 (eqn. (12)), the melting enthalpy of $FeVO_4$ was calculated as 27.8 kJ mol^{-1}.

The DTA curve (Fig. 4) at a low heating rate clearly shows that the mechanisms of oxidation of FeV_2O_4 consists of at least three distinctive processes.

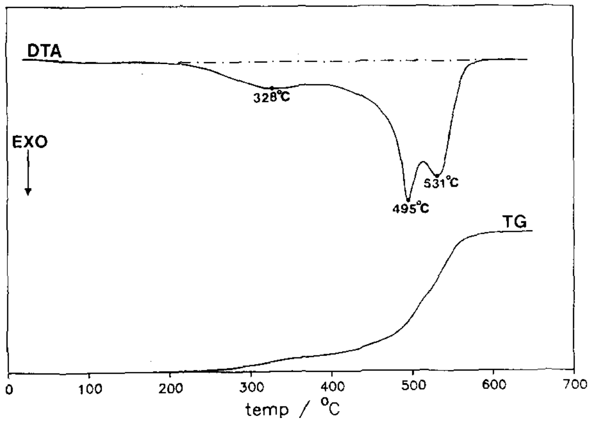

Fig. 4. DTA and TG curves for the oxidation of FeV_2O_4 in O_2 at a heating rate of 5 K min^{-1}.

CONCLUSION

The mechanism of oxidation of FeV_2O_4 is complex, and numerous intermediate reactions take place before V_2O_5 and $FeVO_4$ are formed as final products. The extent of oxidation is influenced by the physical parameter of self-heating.

REFERENCES

1 B. Bunvell, J. Met., 13 (1961) 562.

2 G. Gabra and I. Malivoky, A comparative study of the extraction of vanadium from titaniferous magnetite and slag in H.X. John, N. Carlson and J.T. Smith (Eds.), Extractive Metallurgy of Refractory Metals, TMS-AIME, New York, 1980.

3 A.A. Ryzhov, N.A. Vatolin, P.I. Volkova and V.F. Balakirev, Kinet Catal., 12 (1971) 934.

4 N.A. Vatolin, P.I. Volkova, T.V. Sapozhnikova, N.N. Belyaeva and A.A. Ryzhov, Russ. J. Phys. Chem., 46 (1972) 1538.

5 A. Burdese, Ann. Chim. (Rome) 1, 47 (1957) 817.

6 D.B. Rogers, R.J. Arnott, A. Wold and J.B. Goodenough, J. Phys. Chem. Solids, 24 (1963) 347.

7 M.P. Gupta and H.B. Mathur, J. Phys. C, 8 (1975) 370.

8 E. Riedel and H. Anik, Z. Naturforsch., Teil B, 38 (1983) 1630.

9 A. Baiker, M. Macyevski and A. Reller, Thermochim. Acta, 96 (1985) 81.

10 A.A. Fotiev and V.V. Strelkov, Russ. J. Inorg. Chem. 26 (1981) 942.

11 A. Burdese, Ann. Chim. (Rome) 1, 47 (1957) 817.

12 S.K. Basu and M. Taniguchi, J. Therm. Anal., 29 (1984) 1209.